Drug Development and Industrial Pharmacy, 2011; 37(8): 894–900

ISSN 0363-9045 print/ISSN 1520-5762 online
DOI: 10.3109/03639045.2010.548067

informa
healthcare

RESEARCH ARTICLE

The microstructure characterization of meloxicam microemulsion and its influence on the solubilization capacity

Xiaohui Dong[1], Xue Ke[1], and Zhenggen Liao[2]

[1]Department of Pharmaceutics, China Pharmaceutical University, Nanjing, P. R. China, and [2]Key Laboratory of Modern Preparation of TCM, Ministry of Education, Jiangxi University of Traditional Chinese Medcine, Nanchang,P.R.China

Abstract

Objective: The aim of this study was to characterize the microstructure of microemulsion consisting of oleic acid, Cremophor RH40, ethanol, and water ($K_m = 2$), and investigate the influence of microstructure on the solubilization potential of the microemulsion to meloxicam (MLX).

Methods: Pseudo-ternary phase diagrams of microemulsion were constructed using the H_2O titration method. The microstructures of microemulsion on dilution line N91 were identified by means of conductivity, viscosity, surface tension, and density. The freeze-fracture electron microscopy proved the specific microstructure. Differential scanning calorimetry (DSC) was used to evaluate the position of MLX in microemulsion, and the solubility of MLX in chosen microemulsions on dilution line N91 was measured.

Results: The three microstructures along dilution line N91, including water-in-oil (W/O), bicontinuous (BC), and oil-in-water (O/W) microemulsion, were characterized. The solubilization capacity of W/O microemulsion is the best, compared with the other two, whereas the O/W is the weakest. A possible structure model has been applied for the explanation of difference.

Conclusions: The solubilization capacity of microemulsion is closely related with its microstructure.

Keywords: Microemulsion, microstructure, solubilization, meloxicam, conductivity, viscosity, surface tension and density

Introduction

Microemulsion systems have received increasing attention during the past years[1,2]. As a modern drug carrier system, microemulsions are defined as single optically isotropic and thermodynamically stable solution with droplet sizes in the submicron range[3]. In general, they consist of an oil phase, a surfactant, a cosurfactant, and an aqueous phase[4].

Some advantages offered by microemulsions include improvement in drug solubility, enhancement of bioavailability, protection of the drug against the environment, control of drug release, ease of manufacturing, and a long shelf life[5].

Microemulsions may be envisaged as water-in-oil (W/O) microemulsion, bicontinuous (BC) microemulsion, and oil-in-water (O/W) microemulsion. Many sophisticated physical techniques have been reported for the elucidation of the internal structure of microemulsions[6–9], including dynamic light scattering, electron microscopy, electron paramagnetic resonance (EPR) spectroscopy, pulsed gradient spin echo nuclear magnetic resonance, conductive, viscosity, fluorescence spectroscopy, cyclic voltammetry, small angle neutron scattering. It is possible to determine the microstructure of microemulsions by combining different experimental methods.

The physicochemical characters of microemulsions will change with the microstructure and this will directly affect the use of microemulsions. So, the efficient use of microemulsions in many scientific and industrial applications is directly related to an understanding of their microstructure, which is one of the most basic aspects of microemulsions.

Address for Correspondence: Dr. Xue Ke, Department of Pharmaceutics, China Pharmaceutical University, No. 24 Tong Jia Xiang, Nanjing, 210009, Jiang Su Province, P. R. China. E-mail: kexue1973@vip.sina.com

(Received 09 September 2010; revised 28 November 2010; accepted 12 December 2010)

The one of the purposes of the present contribution was to find and characterize the microstructure of microemulsion composed of oleic acid as the oil phase, Cremophor RH as the surfactant, and an aqueous phase in the presence of cosurfactant (ethanol); the formulation constituents enabled a broad variety of microemulsion compositions, which ranged from water-continuous to oil-continuous aggregates over BC structures.

The second objective of this article was to investigate the influence of microstructure on the solubilization potential of the microemulsions. Meloxicam (MLX) is chosen as a model drug. MLX is a potent nonsteroidal anti-inflammatory drug (NSAID) of the enolic acid class of oxicam derivatives, which shows preferential inhibition of COX-2 and inhibits prostaglandin synthesis[10]. Joint diseases such as rheumatoid arthritis and osteoarthritis can be effectively treated by MLX. Like many NSAIDS, MLX is a hydrophobic drug with practically insoluble in water. The poor solubility leads to poor dissolution and hence varied bioavailability. Thus, increasing the solubility of MLX is of therapeutic importance. Microemulsion is widely used for improving the solubility of MLX[11,12], but little research is about the microstructure on the solubilization capacity of microemulsions.

Materials and methods

Materials

MLX (China Pharmaceutical University Pharmaceutical Co. Ltd., Nanjing, China), Cremophor RH40 (BASF, Germany), oleic acid (Shanghai Lingfeng Biochemical Reagent Co., Ltd., Shanghai, China), methanol was of chromatography pure. All other chemicals and reagents were of AR grade.

HPLC method

The content of MLX in microemulsion was measured by HPLC using a Shidamzu LC-10AT HPLC System. The mobile phase was methanol and 0.1% phosphoric acid solution (65:35, v/v) at a flow rate of 1.0 mL/min with detection at 361 nm. The injection volume is 20 μL.

Preparation of the microemulsion

Based on our previous study, oleic acid was chosen as the oil phase, and the mixed surfactant was Cremophor RH and ethanol with the weight ratio of 2/1. Pseudo-ternary phase diagrams were constructed using the H_2O titration method at ambient temperature to ascertain the concentration range of components for microemulsion. The mixtures of oil and mixed surfactant at certain weight ratio (9/1, 8/2, 7/3, 6/4, 5/5, 4/6, 3/7, 2/8, and 1/9) about 1 g were diluted with aqueous phase dropwise, under moderate agitation. After being equilibrated, the mixtures were assessed visually and determined as being microemulsion. Appearance of turbidity was considered as an indication for phase separation.

Conductive measurement

In the above pseudo-ternary phase diagrams, dilution line N91 (a line in the phase diagram beginning with a mixture of mixed surfactant/oil at a fixed weight ratio of 9/1, which is diluted with water) was chosen for further study. This line was chosen because three microstructures can be found with water dilution.

The conductive measurements were taken by a conductivity meter (DDS-11C; Shanghai Rex Instrument Factory, Shanghai, China). The microemulsion prepared with addition of water was measured after thorough mixing and temperature equilibration at 25°C, the electrode was dipped in the microemulsion sample until equilibrium was reached, and reading becomes stable. Reproducibility was checked for certain samples and no significant differences were observed.

Viscosity measurement

According to the water content from 10% to 90%, we chose nine formulations of microemulsion on the dilution line N91 for viscosity measurement. The microemulsion was placed in a cone-and-plate viscometer (Brookfield Model DV-III ULTRA, Brookfield, WI) and maintained at 25°C. Viscosities were detected at 100 sec^{-1} shear rate with No. 34 rotor. After the level stabilized for 30 sec, the data were recorded. Reproducibility (triplicate) was checked for the samples and no significant differences (±SD) were observed.

Surface tension measurement

Surface tension of above-mentioned microemulsions on dilution line N91 were measured at 25°C with a DCAT 2.1 tensiometer (Dataphysics Instruments GmbH, Germany) using the Wilhemy's plate method. During the measurement, the cleaned platinum plate was dipped into the microemulsion, the pulling force was measured, and then the surface tension was calculated.

Density measurement

Densities of chosen microemulsion on dilution line N91 were measured with weight method. Accurately 5.0 mL of microemulsion was taken at 25°C and calculated for its density. The experiment was repeated for three times.

Morphology

The morphology of microemulsion was observed using freeze-fracture electron microscopy (FFEM) techniques. Three microemulsions on dilution line N91 were chosen; their water contents were 20%, 40%, and 80%, respectively.

The procedure comprised four steps: sample preparation, freezing of the specimen, fracturing and replication, and finally microscopic investigation of the replicas.

First, a small amount of the sample, which was kept at 25°C in a water bath, was rapidly transferred into liquid propane. The sample was clamped under liquid nitrogen inside the vacuum chamber of the freeze-etching apparatus (BAF 400D Freeze-Etching System; Balzers,

Germany) for fracturing. Fracturing was achieved by displacing a microtome arm cooled by liquid nitrogen. The now-exposed fracture face was immediately shadowed. Washing the specimens in THF acid, the replicas were observed with a transmission electron microscope (TECNAI 12; Philip, USA).

Solubility test

The solubility of MLX in the neat components of microemulsion, including oleic acid, Cremophor RH, ethanol, and distilled water, was detected using the shake flask method. In addition, the solubility of MLX in nine microemulsions of dilution line N91 with water content from 10% to 90% was also determined. In brief, an excess amount of MLX was added to each vial containing 5 mL of the selected microemulsion. After sealing, the mixture was vortexed for 10 min in order to facilitate proper mixing of MLX with the microemulsion. Mixtures were shaken for 72 h in an isothermal shaker (Remi, Mumbai, India) maintained at 25 ± 1°C. Mixtures were centrifuged at 12,000 rpm for 10 min; the concentration of MLX in the supernatant was determined by HPLC method.

Differential scanning calorimetry

Three samples were used for differential scanning calorimetric (DSC) measurements: one was a blank BC microemulsion of 40% water on dilution line N91, and the other two were added with MLX in above microemulsion, the final concentrations were 1 and 2 mg/mL, respectively.

DSC measurements were performed with a differential scanning calorimeter Pyris 1 from Perkin-Elmer (San Jose, CA). Nitrogen with a flow of 20 mL/min was used as purge gas. Approximately 10 mg of sample was weighed precisely into a small aluminum pan and quickly sealed hermetically to prevent water evaporation. The empty sealed pan was used as a reference. Samples were cooled to –50°C and held for 5 min, then heated back to 15°C (heating rate: 10°C/min).

Results

Phase diagram

Figure 1 shows the pseudo-ternary phase triangles for the oleic acid/Cremophor RH/ethanol/water system ($K_m = 2$). The isotropic and low-viscosity region is presented in the phase diagram as the one phase microemulsion region.

Electrical conductivity

The electrical conductivity was measured along the dilution line N91 (see phase diagram of Figure 1). Figure 2 displays the influence of water content (Φ) on the electrical conductivity (κ). Initially, the conductivity is very low and a small increase is observed. As the weight fraction of water increases, the electrical conductivity increases rapidly to reach the maximum, then decreases. These changes have been attributed to the occurrence of a percolation transition.

In this percolation model, the conductivity remains low up to a certain fraction of water. It must be emphasized that these conducting W/O droplets, below the percolation threshold, are isolated from each other embedded in non-conducting continuum oil phase and hence contribute very little to the conductance.

However, as the fraction of water reaches the percolation threshold (Φ is about 20%), a fast increase of the conductivity is observed, which indicates that the interaction between the aqueous domains becomes increasingly important and a sticky collision leads to the droplet fusion[13].

The maximum of the curve is close to 70% water, and in this high water content region, the decrease in the conductivity agrees with the mixed micelle formation in an aqueous solution and the aqueous phase becomes the continuous phase, as a structural transition to O/W droplets.

Dynamic viscosity

The understanding of structural consistencies in microemulsions has also been attempted from viscosity

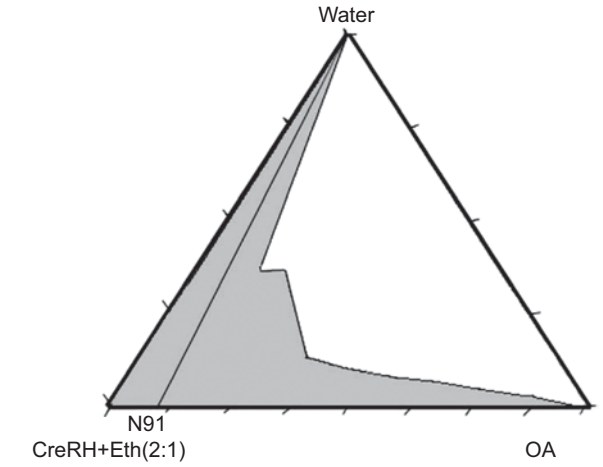

Figure 1. Pseudo-ternary phase diagram of oleic acid/Cremophor RH/ethanol/water ($K_m = 2$) microemulsion system at 25°C; shade region refers to microemulsion.

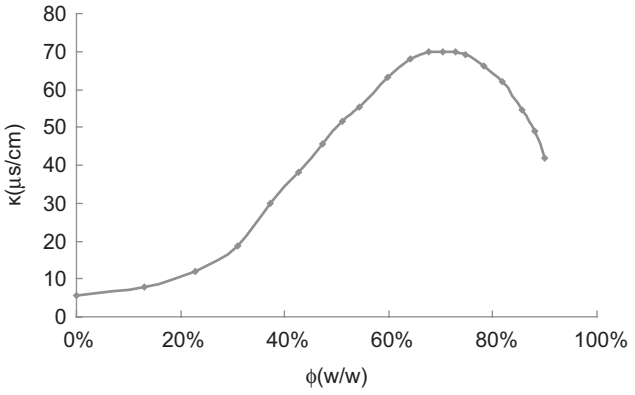

Figure 2. Electrical conductivity as a function of water weight ratio along dilution line N91 in oleic acid/Cremophor RH/ethanol/water ($K_m = 2$) microemulsion at 25°C.

measurements[14–16]. Figure 3 shows the variation in the dynamic viscosity as function of water weight fraction along the dilution line N91.

In the range of water weight fraction below 40%, the gradual increase of viscosity is observed; this suggests that the dispersed phase is present in the form of droplets in the microemulsion systems. The water droplets cluster with the mixed surfactants to form a mixed monomolecular layer of the surfactants couple; they attract each other and aggregate with the increasing water fraction, including molecular reorganization on the interface; and all of these actions increase the viscosity of system.

The viscosity reaches the maxima at 40% water content, and this is an indicative on the transition of microemulsion from a monocontinuous to a BC structure with a labyrinthic network.

After that, the viscosity of the microemulsion continues to decrease; this may be related with the structure of BC microemulsion. Aviram et al.[17] pointed two different BC microstructures as the water dilution progresses. At first, elongated worm-like reverse micelles are dispersed in continuous oil phase; upon further dilution, the microstructure is converted to elongated worm-like direct micelles dispersed in water-continuous phase. The former is called W/O-BC microemulsion and the latter is O/W-BC microemulsion. We assumed that the change of packing pattern of BC microemulsion makes more water molecules free, which leads to the decrease of viscosity.

As the water fraction is above 70%, the dynamic viscosity is very small and unchanged; this is due to the water, which is the least viscous component of the microemulsion system, becomes the outer phase and O/W microemulsions are formed.

Surface tension

Values of surface tension of microemulsion on dilution line N91 versus water weight ratio are presented in Figure 4.

The tension goes up gradually, which is because of the increasing of water with high tension in the microemulsion system. But a slight turning point is shown at 40% water content. The system was stabilized by a surfactant layer that is very flexible and has a zero mean curvature. And it is believed that the phase behavior change of microstructure is responsible for the turning point. At 40% water content, the structure change from droplets with clear interface to misty microtubules composed of oil and water; the interface between oil and water becomes considerable dispersion, which leads to ultralow tension.

Density

The graphical representation of the density data of microemulsion on dilution line N91 is shown in Figure 5.

A sharp increase of density of microemulsion with water weight ratio is observed at earlier stage. This is attributed to the more free surfactant molecules insert inner droplets to form the interfacial monolayer with increasing water; the regular arrangement that leads to the practical volume of microemulsion is less than the ideal value, which corresponds to a sharp increase on density.

The tendency ends up when the water weight ratio is 40%. We assumed that the system may be changed from the isolated W/O droplets to an interconnected BC structure, which makes the most surfactant molecules bound at the interface between oil phase and water phase. Thus the densest packing of microemulsion is formed.

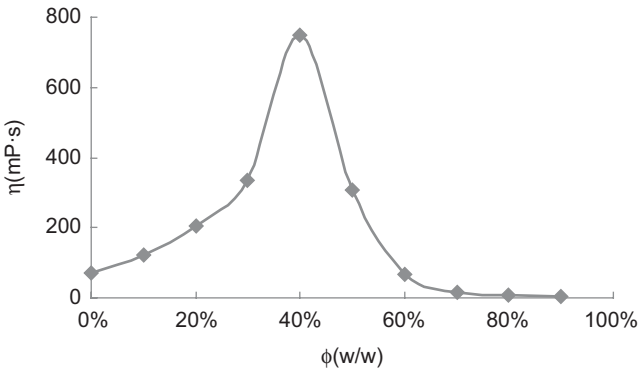

Figure 3. Viscosity as a function of water weight ratio along dilution line N91 of MLX microemulsion at 25°C.

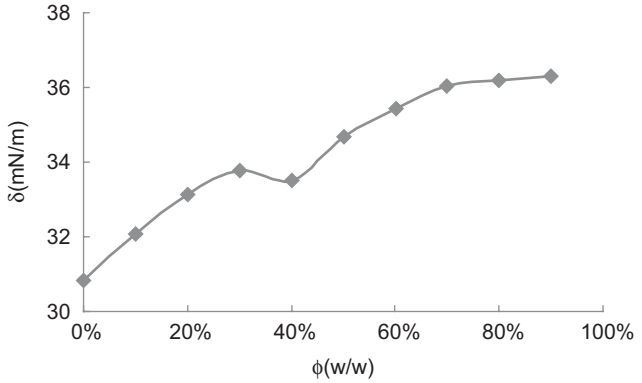

Figure 4. Surface tension as a function of water weight ratio along dilution line N91 of MLX microemulsion at 25°C.

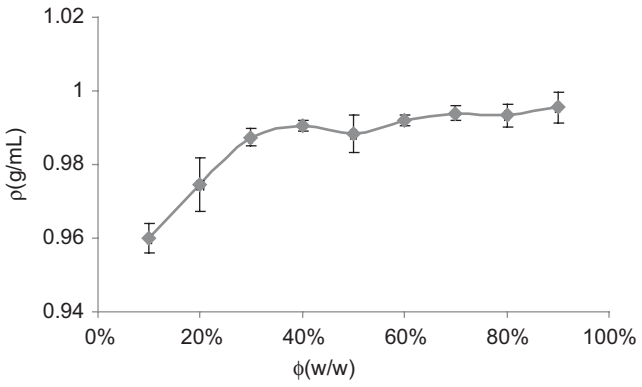

Figure 5. Density as a function of water weight ratio along dilution line N91 of MLX microemulsion at 25°C.

After that, following the increase of water with high density and the decrease of oil and surfactant, the density of microemulsion grows slowly toward the water value (0.997 g/mL).

Comparing the chosen experimental methods, we concluded that the microemulsion composed of oleic acid/Cremophor RH/ethanol/water ($K_m = 2$) on dilution line N91 can be divided into three microstructures: when the water weight ratio is >70%, the microemulsion is expected to be O/W; the water weight ratio below 40% is expected to be oil continuous with isolated water droplets, a W/O microemulsion; finally, a microemulsion that contains roughly between 40% and 70% water will be water as well as oil continuous, a BC microemulsion.

Morphology of microemulsions with different microstructure

The freeze-fracture technique allows observation of the specific structure of different microemulsions as shown in Figure 6.

The water droplets in W/O microemulsion and the oil droplets in O/W microemulsion are sphere and irregular ellipsoid with the size of 10~50 nm.

While, in BC microemulsion, no spherical droplets are observed, the water and oil domains are interwined to form a labyrinthic network; the observed structure is consistent with the picture of BC phases described by Jahn and Strey[18].

Solubility of MLX in neat components of microemulsion

The solubility of MLX in the neat components of microemulsion is shown in Table 1. Similarly in other literatures[19], MLX is practically insoluble in water; even in ethanol, the solubility is very low. But there is higher solubility in the oil phase and surfactant, especially in surfactant. The solubility of MLX in surfactant is about 400 times compared with water phase, and about four times compared with oil phase.

DSC measurements

Here, DSC is used to obtain information about the position of MLX in microemulsion for further interpretation about solubilization capacity. Figure 7 shows typical DSC curves containing 0, 1, 2 mg of MLX in 1 mL microemulsion.

There are two peaks in the curve: the left broad peak is about from –10°C to –40°C and right small peak is about from –10°C to 0°C. In view of the melting point of oleic acid that is 16.3°C, the two peaks should correspond to the other component in microemulsion.

In general, there exist three forms of water molecule in microemulsion: free or bulk water (melting point: around 0°C), interfacial water (melting point: around –10°C), and bound water (melting point: below –10°C)[20]. So, the right peak around –7°C in DSC curves should be indicative of interfacial water.

According to the literatures[21], the left peak may be related to the melting of the interface monolayer consisting of Cremophor RH and ethanol between the water and oil phases.

With increasing amounts of MLX, the left peak moves toward higher temperatures from –29.8°C to –21.3°C, and at the same time, the enthalpy increases from 2.88 to 3.89 J/g. On the other hand, right peak, which is attributed to interfacial water, does not change with the addition of MLX. This indicates that the existence of MLX has influence on the interface film of surfactant, but has no relationship with water phase. Combining the higher solubility of MLX in surfactant (listed in Table 1), we assumed that MLX in microemulsion is present at the interface that composed of Cremophor RH and ethanol. Considering the hydrophobicity of the drug molecule, MLX at the interface film tend to insert in the hydrocarbon chain of Cremophor RH.

Solubility of MLX in microemulsion

The solubility of MLX in the chosen microemulsions is shown in Table 2. We also calculated the linear relationship between the solubility (S) and water weight ratio (Φ)

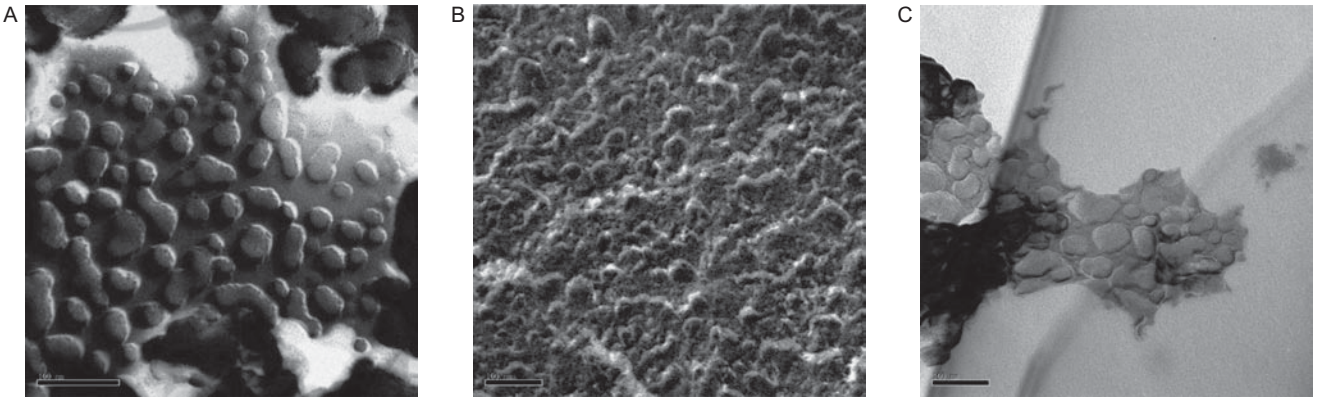

Figure 6. Image of the freeze-fractured microemulsions with three kinds of microstructures. A is W/O microemulsion, B is BC microemulsion, and C is O/W microemulsion.

in three microstructure region, and the equations were listed in Table 2.

Relationship between microstructure of microemulsion and solubilization capacity for MLX

According to the above result, we have some conclusions. First, the solubility of MLX in microemulsion apparently increases from about 10 times to 290 times, compared with the original 0.02 mg/mL in water. This proves the solubilization properties of microemulsion to insoluble drug.

Second, the solubilization capacity of microemulsion is related with the microstructure. Among them, W/O and BC microemulsion may be the better choice for the solubilization of MLX, while the solubilization capacity of O/W microemulsion is limited.

Table 1. The solubility of MLX in each component of microemulsion ($n=3$).

Component	Solubility (mg/mL)
Oleic acid	2.01 ± 0.06
Cremophor RH	7.86 ± 0.43
Ethanol	0.47 ± 0.08
Water	0.02 ± 0.01

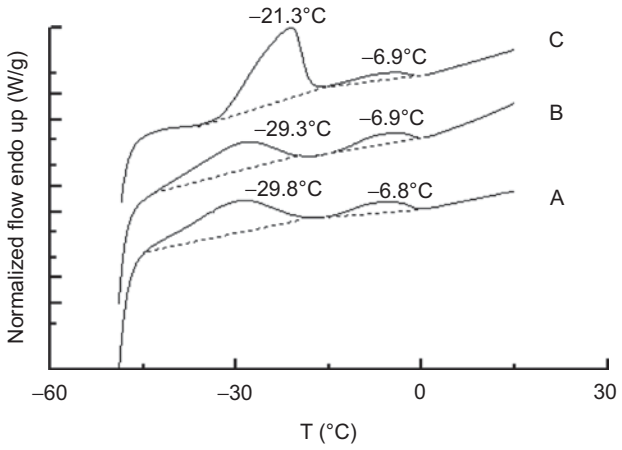

Figure 7. DSC curves of MLX microemulsion. A refers to blank microemulsion, B refers to 1 mg/mL MLX microemulsion, and C refers to 2 mg/mL MLX microemulsion.

Although this phenomenon can be partly explained from the solubility of MLX in oil phase and surfactant higher than in water, we indeed noticed that the increase of solubility among three microstructure regions shows a nonlinear pattern from the different coefficient of each equation listed in Table 2.

We think the microstructure and the position of drug molecule in microemulsion may play the important role in deciding the solubilization capacity to MLX.

For instance, in O/W microemulsion, the hydrophobic hydrocarbon chain of surfactant, which is main packing position of MLX in microemulsion, is confined in the inner of oil droplets; the restricted configuration of the chain leads to no enough space for the embedding of MLX (the schematic illustration in Figure 8C). So, following the decrease in water ratio (i.e. the ratio of surfactant is increasing), theoretically more O/W droplets are produced, which is of advantage in increasing solubility, but in fact, the restricted mechanism of solubilization makes the solubility of MLX increase very slowly.

When the O/W microemulsion enters in the BC region, the system changes from isolated droplets to a labyrinthic network; the closely packed structure of surfactant's lipophilic tail is partly released, which has more space to accommodate the MLX molecules (see Figure 8B). Thus, the increase of solubility in the region is faster.

Along the W/O microstructure, the solubility of MLX is found to increase continuously with water content

Table 2. Solubility of MLX in microemulsion on dilution line N91 with different microstructures at 37°C ($n=3$).

Microstructure	Water ratio (%)	Solubility (mg/mL)	Equation between solubility and water weight ratio
	10	5.85 ± 0.39	
W/O	20	4.41 ± 0.59	$S=-15.4\varphi+7.5$
	30	2.76 ± 0.57	$R^2=0.99$
	40	1.79 ± 0.26	
BC	50	1.05 ± 0.14	$S=-6.0\varphi+4.1$
	60	0.59 ± 0.01	$R^2=0.98$
	70	0.40 ± 0.02	
O/W	80	0.26 ± 0.01	$S=-1.0\varphi+1.1$
	90	0.20 ± 0.01	$R^2=0.95$

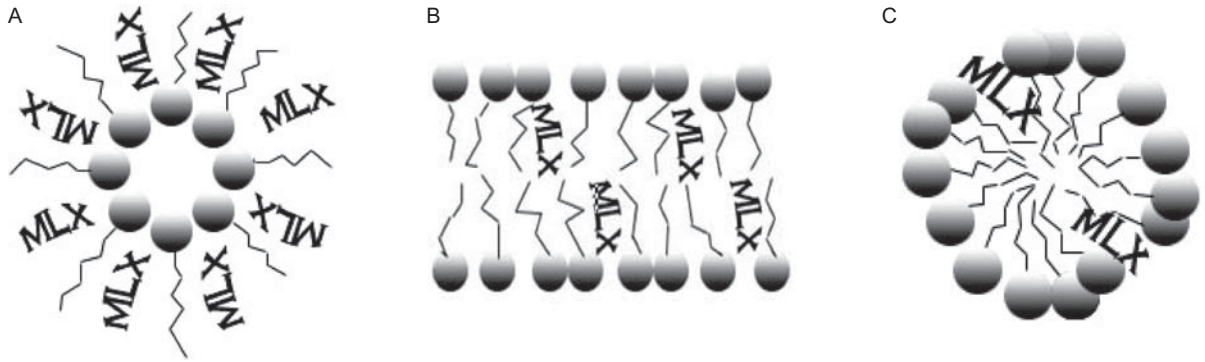

Figure 8. Schematic representation of microemulsion microstructure and MLX packing pattern. A is W/O microemulsion, B is BC microemulsion, and C is O/W microemulsion.

decreasing, and a steepest slope in three microemulsions. This can be seen in Figure 8A; due to the unlimited hydrophobic chains of the surfactant, enough space is produced for MLX molecules' penetration into the interfacial film.

Discussion

The microstructures of a microemulsion incorporating oleic acid, Cremophor RH, ethanol, and water ($K_m = 2$) are studied and identified. By means of conductivity, viscosity, surface tension, and density test, the microemulsion on dilution line N91 is found to transfer from W/O to BC and final O/W upon water dilution. The freeze-fracture technique further observes the specific structure of different microemulsions.

The solubility results reveal that the solubilization capacity of microemulsion to MLX increased from O/W to BC and W/O. The analysis of the results indicates that the difference is related not only with the proportion of each component in microemulsion, but also with the microstructure of microemulsion.

Additional DSC test, combined the obvious solubility difference of MLX in each component of microemulsion, indicate that MLX molecules mainly accommodate at the interfacial film of microemulsion composed of surfactant and cosurfactant. Based on the results, a possible mechanism about the difference in solubilization capacity among three microstructures of microemulsion is proposed in the present study.

Although the different microstructures indeed influence the solubilization capacity of microemulsion, the factor affecting the usage of microemulsion is multifaceted, for example, W/O microemulsion is commonly inferior to O/W in the percutaneous characteristics. So, besides the solubilization capacity, more considerations should be made in choosing appropriate microemulsion for pharmaceutical use.

Declaration of interest

This study was supported by the Major Project of National Science and Technology of China for New Drugs Development (No. 2009ZX09310-004)

References

1. Tenjarla S. (1999). Microemulsions: an overview and pharmaceutical applications. Crit Rev Ther Drug Carrier Syst, 16:461–521.
2. Bagwe RP, Kanicky JR, Palla BJ, Patanjali PK, Shah DO. (2001). Improved drug delivery using microemulsions: rationale, recent progress, and new horizons. Crit Rev Ther Drug Carrier Syst, 18:77–140.
3. Lee PJ, Langer R, Shastri VP. (2003). Novel microemulsion enhancer formulation for simultaneous transdermal delivery of hydrophilic and hydrophobic drugs. Pharm Res, 20:264–269.
4. Rhee YS, Choi JG, Park ES, Chi SC. (2001). Transdermal delivery of ketoprofen using microemulsions. Int J Pharm, 228:161–170.
5. Paul BK, Moulik SP. (2001). Uses and applications of microemulsions. Curr Sci, 80:990–1001.
6. Podlogar F, Gasperlin M, Tomsic M, Jamnik A, Rogac MB. (2004). Structural characterisation of water–Tween 40/Imwitor 308–isopropyl myristate microemulsions using different experimental methods. Int J Pharm, 276:115–128.
7. Fanun M. (2008). Phase behavior, transport, diffusion and structural parameters of nonionic surfactants microemulsions. J Mol Liquids, 139:14–22.
8. Sripriya R, Muthu Raja K, Santhosh G, Chandrasekaran M, Noel M. (2007). The effect of structure of oil phase, surfactant and co-surfactant on the physicochemical and electrochemical properties of bicontinuous microemulsion. J Colloid Interface Sci, 314:712–717.
9. de Campo L, Yaghmur A, Garti N, Leser ME, Folmer B, Glatter O. (2004). Five-component food-grade microemulsions: structural characterization by SANS. J Colloid Interface Sci, 274:251–267.
10. Luger P, Daneck K, Engel W, Trummlitz G, Wagner K. (1996). Structure and physicochemical properties of meloxicam, a new NSAID. Eur J Pharm Sci, 4:175–187.
11. Yuan Y, Li S-M, Yu L-M, Deng P, Zhong D-F. (2007). Physicochemical properties and evaluation of microemulsion systems for transdermal delivery of meloxicam. Chem Res Chin Univ, 23:81–86.
12. Yuan Y, Li S-M, Mo F-K, Zhong D-F. (2006). Investigation of microemulsion system for transdermal delivery of meloxicam. Int J Pharm, 321:117–123.
13. Moulik SP, Paul BK. (1998). Structure, dynamics and transport properties of microemulsions. Adv Colloid Interface Sci, 78:99–195.
14. Mehta SK, Bala K. (2000). Tween-based microemulsions: a percolation view. Fluid Phase Equilibria, 172:197–209.
15. Ezrahi S, Aserin A, Garti N. (1998). Structural evolution along water dilution lines in nonionic systems. J Colloid Interface Sci, 203:222–224.
16. Djordjevic L, Primorac M, Stupar M, Krajisnik D. (2004). Characterization of caprylocaproyl macrogolglycerides based microemulsion drug delivery vehicles for an amphiphilic drug. Int J Pharm, 271:11–19.
17. Spernath A, Aserin A, Sintov AC, Garti N. (2008). Phosphatidylcholine embedded micellar systems: enhanced permeability through rat skin. J Colloid Interface Sci, 318:421–429.
18. Jahn W, Strey R. (1988). Microstructure of microemulsions by freeze fracture electron microscopy. J Phys Chem, 92:2294–301.
19. Vijaya Kumar SG, Zasshi DY. (2006). Preparation, characterization and *in vitro* dissolution studies of solid dispersion of meloxicam with PEG6000. J Pharm Soc Jpn, 126:657–664.
20. Note C, Koetz J, Kosmella S. (2006). Structural changes in poly(ethyleneimine) modified microemulsion. J Colloid Interface Sci, 302:662–668.
21. Fujieda T, Ohta K, Wakabayashi N, Higuchi S. (1997). H-aggregation of methyl orange at the interface between the water phase and oil phase in a water-in-oil microemulsion. J Colloid Interface Sci, 185:332–334.